

Membrane Fusion-Based Transmitter Design for Molecular Communication Systems

Xinyu Huang*, Yuting Fang[†], Adam Noel[‡], and Nan Yang*

*School of Engineering, Australian National University, Canberra, ACT, Australia

[†]Department of Electrical and Electronic Engineering, University of Melbourne, Parkville, VIC, Australia

[‡]School of Engineering, University of Warwick, Coventry, CV4 7AL, UK

Email: xinyu.huang1@anu.edu.au, yuting.fang@unimelb.edu.au, adam.noel@warwick.ac.uk, nan.yang@anu.edu.au

Abstract—This paper proposes a novel imperfect spherical transmitter (TX) model, namely the membrane fusion (MF)-based TX, that adopts MF between a vesicle and the TX membrane to release molecules encapsulated within the vesicle. For the MF-based TX, the molecule release probability and the fraction of molecules released from the TX membrane are derived. Incorporating molecular degradation and a fully-absorbing receiver (RX), the end-to-end molecule hitting probability at the RX is also derived. A simulation framework for the MF-based TX is proposed, where the released point on the TX membrane and the released time of each molecule are determined. Aided by the simulation framework, the derived analytical expressions are validated. Simulation results verify that a low MF probability or low vesicle mobility slows the release of molecules from the TX, extends time required to reach the peak release probability, and reduces the end-to-end molecule hitting probability at the RX.

Index Terms—Molecular communication, imperfect transmitter design, membrane fusion, release probability, diffusion

I. INTRODUCTION

Molecular communication (MC) has become one of the most promising methods for nanoscale communication. In MC, molecules act as information carriers. The main driving force behind engineering MC is its diversity of potential applications in the medical field, e.g., lab-on-a-chip devices, cell-on-chip devices, and targeted drug delivery [1]. An end-to-end MC channel model incorporates a transmitter (TX), the propagation environment, and a receiver (RX). Molecule propagation environment and reception mechanism at the RX have been widely investigated in previous studies, e.g., [2], [3]. However, few studies have investigated the impact of signaling pathways inside the TX and the interaction of molecular signals with the TX surface on the MC system performance.

Most existing studies assumed the TX to be an ideal point source that can release molecules instantaneously [3]. Compared to realistic scenarios, this ideal TX neglects the effects of TX geometry, signaling pathways inside the TX, and chemical reactions during the release process. Recently, some studies considered these effects of the TX, e.g., [4]–[6]. [4] proposed a spherical TX that reflects the emitted molecules and investigated the directivity gain achieved by the reflecting TX. [5] proposed an ion channel based TX, where molecule release is controlled by opening and closing ion channels. [6] considered a spherical TX with a semi-permeable boundary whose permeability is used to control molecule release. Although these studies stand on their own merits, none of them

has considered an exocytosis-like mechanism for molecule release.

In nature, exocytosis is a form of active transport in which a cell transports molecules out of the cell by secreting them through an energy-dependent process [7]. Exocytosis is common for cells because many chemical substances are large molecules and cannot pass through the cell membrane by passive means [8]. In exocytosis, vesicles¹ are carried to the cell membrane to secrete their contents into the extracellular environment. This secretion is performed by the membrane fusion (MF) that fuses the vesicle with the cell membrane. When the vesicle moves close to the cell membrane, the v-SNARE protein on the vesicle membrane binds to the t-SNARE protein on the cell membrane to generate the *trans*-SNARE complex that catalyzes MF [9]. Unlike the ideal point TX, exocytosis constraints the release of molecules. Hence, a TX that uses MF to release molecules merits investigation.

In this paper, we propose a novel TX model in a three-dimensional (3D) environment, namely the MF-based TX, which uses fusion between a vesicle generated within the TX and the TX membrane to release molecules encapsulated within the vesicle. By considering a fully-absorbing RX that absorbs molecules once they hit the RX surface, we investigate the end-to-end channel impulse response (CIR) between the MF-based TX and the RX, where the CIR is the hitting probability of molecules at the RX [3].

Our major contributions are summarized as follows. We first derive the time-varying molecule release probability and the fraction of molecules released from the TX by a given time. We then derive the end-to-end molecule hitting probability at the RX due to the MF-based TX. Furthermore, we propose a simulation framework for the MF-based TX model to simulate the diffusion and fusion of vesicles within the TX. In this simulation framework, the release point on the TX membrane and the release time of each molecule are determined. Aided by the proposed simulation framework, we demonstrate the accuracy of our analytical derivations. Our numerical results show that a low MF probability or low vesicle mobility slows the release of molecules from the TX, increases the time to reach the peak release probability, and reduces the end-to-end

¹A vesicle is a small, round or oval-shaped container for the storage of molecules, and as compartments with particular chemical reactions [9].

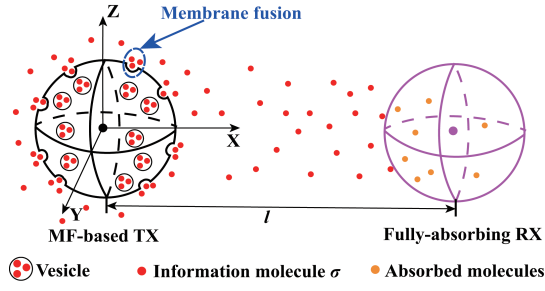


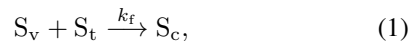
Fig. 1. Illustration of the system model, where one MF-based TX communicates with one fully-absorbing RX in a 3D environment.

molecule hitting probability at the RX.

II. SYSTEM MODEL

In this paper, we consider an unbounded 3D environment, where an MF-based TX communicates with a fully-absorbing RX, as depicted in Fig. 1. Both TX and RX are spheres with radius r_T and r_R , respectively. The center of the TX is chosen as the origin of the environment. The center of the RX is distance l away from the center of the TX. We assume that the spherical TX releases molecules from its outer membrane after fusion between the membrane and vesicles. Each vesicle stores and transports η molecules of type σ . We consider that the TX is filled with a fluid medium that has uniform temperature and viscosity. We also consider an impulse of N_v vesicles released within the TX at $t = 0$. The experiment in [10] demonstrates that vesicles diffuse in a fluid medium with a diffusion coefficient. Based on [10], we assume that once vesicles are released, they diffuse randomly with a constant diffusion coefficient D_v . According to [9], natural fusion of a vesicle and the cell membrane can be considered as two steps: 1) The v-SNARE protein (S_v) on the vesicle membrane binds to the t-SNARE protein (S_t) on the cell membrane to generate the *trans*-SNARE complex (S_c), and 2) S_c catalyzes the fusion of vesicular and cell membranes. For tractability, we make the following assumptions on the TX model:

- A1) Vesicles are released from the TX's center. This assumption simplifies the theoretical analysis since the TX model is symmetrical. Considering vesicles released from any point within the TX is an interesting future work.
- A2) The binding between S_v and S_t is modeled as an irreversible reaction, given by



where k_f is the forward reaction rate in $\mu\text{m/s}$. We acknowledge that the MF process in nature is more complex than this assumption. For instance, MF also depends on an increased intracellular calcium (Ca^{2+}) concentration [11]. The irreversible reaction modeled in (1) is a good first step to incorporate the MF mechanism in MC modeling.

- A3) The membrane is fully covered by an infinite number of S_t and the occupancy of S_t is ignored. Assuming perfect receptor coverage and ignoring occupancy are for

tractability and have been adopted in several previous studies, e.g., [2], [12].

- A4) The generation of S_c guarantees MF. In nature, S_c catalyzes the MF process. Hence, this assumption becomes reasonable if the reaction rate of this catalytic reaction is assumed to be infinity.
- A5) Once molecules are released, the spherical TX does not hinder the random diffusion of molecules in the propagation environment, i.e., the TX is transparent to the diffusion of released molecules. [4] analyzed the hindrance of the TX membrane to the diffusion of molecules using simulation. Considering both the hindrance of the TX membrane and the absorbing RX is cumbersome for theoretical analysis. We will investigate the impact of the TX membrane on molecule diffusion in the propagation environment in future work.

Based on A2-A4, if a vesicle hits the TX membrane, it fuses to the membrane with a probability of $k_f \sqrt{\frac{\pi \Delta t}{D_v}}$ during a time interval Δt [13]. We define this probability as the MF probability. After MF, the molecules σ stored by the vesicle are released into the propagation environment. The location and time for the occurrence of MF are the initial location and time for molecules to start moving in the propagation environment.

We assume that the propagation environment outside the spherical TX and RX is a fluid medium with uniform temperature and viscosity. Once information molecules σ are released from the TX, they diffuse randomly with a constant diffusion coefficient D_σ . Moreover, we consider unimolecular degradation in the propagation environment, where type σ molecules can degrade into some other molecular species $\hat{\sigma}$ that cannot be identified by the RX, i.e., $\sigma \xrightarrow{k_d} \hat{\sigma}$ [14, Ch. 9], where k_d [s^{-1}] is the degradation rate. In addition, we model the RX as a spherical fully-absorbing RX. Molecules σ are absorbed as soon as they hit the RX surface.

III. DERIVATION OF CHANNEL IMPULSE RESPONSE

In this section, we first derive the molecule release probability and the fraction of released molecules from the TX membrane due to the impulsive emission of vesicles from the TX's center. We define the molecule release probability as the probability of one molecule being released at time t from the TX membrane, when this molecule is released from the origin at time $t = 0$. We then derive the molecule hitting probability at the RX when the TX releases molecules uniformly over the TX membrane. We define the molecule hitting probability as the probability of one molecule hitting the RX at time t when this molecule is released at time $t = 0$. Using the previously derived release probability and hitting probability, we finally derive the end-to-end molecule hitting probability at the RX due to the impulsive emission of vesicles from the TX's center.

A. Release Probability from TX Membrane

As each molecule is released when MF occurs, the molecule release probability equals the fusion probability of vesicles. Thus, we need to obtain the distribution function of vesicles within the TX to derive the molecule release probability from

the TX membrane. In the spherical coordinate system, we denote $C(r, t)$, $0 \leq r \leq r_T$, as the vesicle distribution function at time t with distance r from the TX's center. When an impulse of vesicles is released from the TX's center at $t = 0$, the initial condition is expressed as [15, eq. 3(c)]

$$C(r, t \rightarrow 0) = \frac{1}{4\pi r^2} \delta(r), \quad (2)$$

where $\delta(\cdot)$ is the Dirac delta function. According to Fick's second law, the diffusion of vesicles inside the TX can be described as [16]

$$D_V \frac{\partial^2 (rC(r, t))}{\partial r^2} = \frac{\partial (rC(r, t))}{\partial t}. \quad (3)$$

Based on A2 and A4, the boundary condition is described by the irreversible reaction given by (1), which can be characterized by the third type (Robin) boundary condition as [17]

$$D_V \frac{\partial C(r, t)}{\partial r} \Big|_{r=r_T} = -k_f C(r_T, t), \quad (4)$$

where the negative sign on the right-hand side indicates that the condition is over the inner boundary.

Based on the initial condition in (2), Fick's second law in (3), and the boundary condition in (4), we derive the closed-form expression for the release probability from the TX membrane, denoted by $f_r(t)$, in the following theorem:

Theorem 1: The release probability of molecules from the TX membrane at time t is given by

$$f_r(t) = \sum_{n=1}^{\infty} \frac{4r_T^2 k_f \lambda_n^3}{2\lambda_n r_T - \sin(2\lambda_n r_T)} j_0(\lambda_n r_T) \exp(-D_V \lambda_n^2 t), \quad (5)$$

where $j_0(\cdot)$ is the zeroth order of the first type of the spherical Bessel function [18], $n = 1, 2, 3, \dots$, and λ_n is obtained by solving

$$D_V \lambda_n j_0'(\lambda_n r_T) = -k_f j_0(\lambda_n r_T), \quad (6)$$

where $j_0'(z) = \frac{\partial j_0(z)}{\partial z}$.

Proof: Please see Appendix A. ■

We denote $F_r(t)$ as the fraction of molecules released by time t and obtain it by $F_r(t) = \int_0^t f_r(u) du$. We present $F_r(t)$ in the following corollary:

Corollary 1: The fraction of released molecules from the TX by time t is given by

$$F_r(t) = \sum_{n=1}^{\infty} \frac{4r_T^2 k_f \lambda_n j_0(\lambda_n r_T)}{D_V (2\lambda_n r_T - \sin(2\lambda_n r_T))} (1 - \exp(-D_V \lambda_n^2 t)). \quad (7)$$

The number of molecules released by time t is $N_V \eta F_r(t)$.

B. Hitting Probability at RX with Uniform Release of Molecules

The aim of this paper is to derive the end-to-end hitting probability of molecules at the RX surface when an impulse of vesicles is released from the TX's center. To this end, we first derive the hitting probability when the molecules

are uniformly released from the TX membrane, i.e., ignoring the internal molecules' propagation within the TX and the TX MF process. We consider the scenario that molecules are initially uniformly distributed over the TX membrane and released simultaneously at $t = 0$, where the membrane area is denoted by Ω_T . We denote $p_u(t)$ as the corresponding hitting probability at the RX due to the uniform release of molecules over the TX membrane. We note that uniformly-distributed molecules means that the likelihood of a molecule released from any point on the TX membrane is the same. We denote this probability by ρ , where we have $\rho = (4\pi r_T^2)^{-1}$. We further consider an arbitrary point α on the TX membrane. Based on [19, eq. (9)], the hitting probability $p_\alpha(t)$ of a molecule at the RX at time t when the molecule is released from the point α at time $t = 0$ is given by

$$p_\alpha(t) = \frac{r_R(l_\alpha - r_R)}{l_\alpha \sqrt{4\pi D_\sigma t^3}} \exp\left(-\frac{(l_\alpha - r_R)^2}{4D_\sigma t} - k_d t\right), \quad (8)$$

where l_α is the distance between the point α and the center of the RX.

Given that molecules are distributed uniformly over the TX membrane, $p_u(t)$ is obtained by taking the surface integral of $p_\alpha(t)$ over the spherical TX membrane. Using this method, we solve $p_u(t)$ in the following lemma:

Lemma 1: The hitting probability of molecules at the RX at time t when the TX uniformly releases the molecules over the TX membrane at time $t = 0$ is given by

$$p_u(t) = \frac{2\rho r_T r_R}{l} \sqrt{\frac{\pi D_\sigma}{t}} \left[\exp\left(-\frac{\beta_1}{t} - k_d t\right) - \exp\left(-\frac{\beta_2}{t} - k_d t\right) \right], \quad (9)$$

where $\beta_1 = \frac{(r_T + r_R)(r_T + r_R - 2l) + l^2}{4D_\sigma}$ and $\beta_2 = \frac{(r_T - r_R)(r_T - r_R + 2l) + l^2}{4D_\sigma}$.

Proof: Please see Appendix B. ■

C. End-to-End Hitting Probability at the RX

We denote $p_v(t)$ as the end-to-end hitting probability of molecules at the RX when an impulse of vesicles is released from the TX's center at time $t = 0$. The release probability of molecules from the TX at time u , $0 \leq u \leq t$, is given by (5), which is $f_r(u)$. For molecules released at time u , the hitting probability of molecules at the RX at time t is given by (9), which is $p_u(t - u)$. Based on that, $p_v(t)$ is given by

$$p_v(t) = \int_0^t p_u(t - u) f_r(u) du. \quad (10)$$

Substituting (5) and (9) into (10), we derive $p_v(t)$ in the following theorem:

Theorem 2: The end-to-end hitting probability of molecules at the RX at time t for an impulsive emission of vesicles from the TX's center at time $t = 0$, is given by

$$p_v(t) = \frac{8\rho r_T^3 r_R k_f \sqrt{\pi D_\sigma} \exp(-k_d t)}{l} \sum_{n=1}^{\infty} \frac{\lambda_n^3 j_0(\lambda_n r_T)}{2\lambda_n r_T - \sin(2\lambda_n r_T)} \times [\varepsilon(\beta_1, t) - \varepsilon(\beta_2, t)], \quad (11)$$

where

$$\varepsilon(\zeta, t) = \int_0^t \frac{1}{\sqrt{t-u}} \exp\left(-\frac{\zeta}{t-u} - (D_v \lambda_n^2 - k_d)u\right) du. \quad (12)$$

$\varepsilon(\zeta, t)$ can be calculated numerically using the MATLAB.

IV. SIMULATION FRAMEWORK FOR MF-BASED TX

In this section, we describe the stochastic simulation framework for the MF-based TX. We use a particle-based simulation method that records the exact position of each vesicle. For simulating molecules' diffusion in the propagation environment and absorption by the RX, the particle-based simulation is also applied, which is omitted here due to the page limit.

A. Emission and Diffusion

N_v vesicles are released from the TX's center at $t = 0$. We denote Δt_s as the simulation interval. After vesicles are released, they perform Brownian motion during each simulation interval. Therefore, the displacements of each vesicle in three dimensions during the simulation interval are independent Gaussian random variables (RVs) with zero mean and variance $2D_v \Delta t_s$.

B. Fusion or Reflection

We denote the locations of a vesicle at the start and end of the γ th simulation interval by $(x_{\gamma-1}, y_{\gamma-1}, z_{\gamma-1})$ and $(x_\gamma, y_\gamma, z_\gamma)$, respectively. If the distance between a vesicle and the TX's center is larger than r_T at the end of the γ th interval, we assume that the vesicle has hit the TX membrane. As described in Section II, this vesicle then fuses with the TX membrane with probability $k_f \sqrt{\frac{\pi \Delta t_s}{D_v}}$ and is reflected with probability $1 - k_f \sqrt{\frac{\pi \Delta t_s}{D_v}}$.

Molecules stored in a vesicle are released at the time and location where the vesicle fused with the TX membrane. Thus, we need to derive where and when fusion with the membrane occurred. For a vesicle fusing with the TX membrane during the γ th simulation interval, we assume that the intersection between the line that is formed by $(x_{\gamma-1}, y_{\gamma-1}, z_{\gamma-1})$ and $(x_\gamma, y_\gamma, z_\gamma)$ and the TX membrane is the fusion point whose coordinates, denoted by $(x_{f,\gamma}, y_{f,\gamma}, z_{f,\gamma})$, are given by [20]

$$x_{f,\gamma} = \frac{-\Lambda_2 \pm \sqrt{\Lambda_2^2 - 4\Lambda_1\Lambda_3}}{2\Lambda_1}, \quad (13)$$

$$y_{f,\gamma} = \frac{(x_{f,\gamma} - x_{\gamma-1})(y_\gamma - y_{\gamma-1})}{x_\gamma - x_{\gamma-1}} + y_{\gamma-1}, \quad (14)$$

and

$$z_{f,\gamma} = \frac{(x_{f,\gamma} - x_{\gamma-1})(z_\gamma - z_{\gamma-1})}{x_\gamma - x_{\gamma-1}} + z_{\gamma-1}, \quad (15)$$

respectively, where $\Lambda_1 = (x_\gamma - x_{\gamma-1})^2 + (y_\gamma - y_{\gamma-1})^2 + (z_\gamma - z_{\gamma-1})^2$, $\Lambda_2 = 2(y_\gamma - y_{\gamma-1})(x_\gamma y_{\gamma-1} - x_{\gamma-1} y_\gamma) + 2(z_\gamma - z_{\gamma-1})(x_\gamma z_{\gamma-1} - x_{\gamma-1} z_\gamma)$, and $\Lambda_3 = x_{\gamma-1}(y_\gamma - y_{\gamma-1})(x_{\gamma-1} y_\gamma - 2y_{\gamma-1} x_\gamma + y_{\gamma-1} x_\gamma) + x_{\gamma-1}(z_\gamma - z_{\gamma-1})(x_{\gamma-1} z_\gamma - 2x_\gamma z_{\gamma-1} + x_{\gamma-1} z_{\gamma-1}) + (x_\gamma - x_{\gamma-1})^2 (y_{\gamma-1}^2 + z_{\gamma-1}^2 - r_T^2)$. In (13), $x_{f,\gamma}$ is chosen by satisfying $(x_{f,\gamma} -$

$x_{\gamma-1})(x_{f,\gamma} - x_\gamma) < 0$. We denote $t_{\gamma-1}$ as the start time of the γ th simulation interval and $t_{\gamma-1} + \Delta t_{f,\gamma}$ as the fusion time of the vesicle in the γ th simulation interval. As each vesicle follows Brownian motion, the square of the displacement is proportional to the time within the same simulation interval. Therefore, we derive $\Delta t_{f,\gamma}$ as

$$\Delta t_{f,\gamma} = \frac{(x_{f,\gamma} - x_{\gamma-1})^2 + (y_{f,\gamma} - y_{\gamma-1})^2 + (z_{f,\gamma} - z_{\gamma-1})^2}{(x_\gamma - x_{\gamma-1})^2 + (y_\gamma - y_{\gamma-1})^2 + (z_\gamma - z_{\gamma-1})^2} \Delta t_s. \quad (16)$$

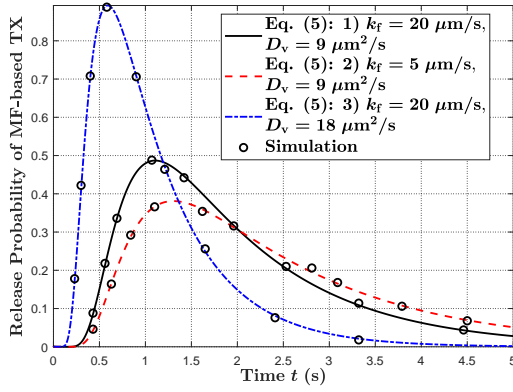
For vesicles failing to fuse with the TX membrane, we make the assumption that they are sent back to their positions at the start of the current simulation interval.

V. NUMERICAL RESULTS AND DISCUSSIONS

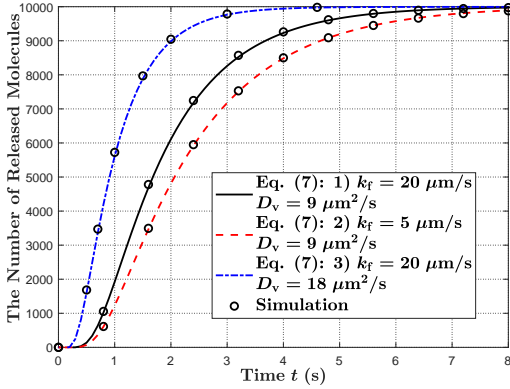
In this section, we present numerical results to validate our theoretical analysis and enable insightful discussion. The simulation time interval is $\Delta t_s = 0.001$ s and all results are averaged over 5000 realizations. Throughout this section, we set $N_v = 100$, $\eta = 100$, $r_T = r_R = 10$ μm , $D_v = 9$ $\mu\text{m}^2/\text{s}$, $k_f = 20$ $\mu\text{m}/\text{s}$, $l = 40$ μm , $k_d = 0.8$ s^{-1} , and $D_\sigma = 1000$ $\mu\text{m}^2/\text{s}$ [10], [12], unless otherwise stated. In Figs. 2-4, we vary the forward reaction rate and vesicle diffusion coefficient to investigate their impact on molecule release, time to reach the peak release probability, and molecule absorption. In Fig. 2 and Fig. 4, we observe precise agreement between our simulation results and the analytical curves generated from Section III, which demonstrate the accuracy of our analysis.

In Fig. 2, we plot the molecule release probability from the TX at time t versus time t in Fig. 2(a) and the number of released molecules from the TX until time t versus time t in Fig. 2(b). First, by comparing parameter sets 1) and 2) in Fig. 2(a), we observe that the peak release probability decreases and the tail of the release probability becomes longer with a decrease in k_f . This is because the decrease in k_f reduces the fusion probability between a vesicle and the TX membrane. Second, by comparing parameter sets 1) and 3) in Fig. 2(a), we observe that the peak release probability decreases and a longer time is required for the TX to start releasing molecules with a decrease in D_v . This is because decreasing D_v slows down the vesicle. Third, in Fig. 2(b), we observe that all molecules are released from the TX with sufficient long time due to the impulsive release.

In Fig. 3, we plot the time to reach the peak molecule release probability from the TX, denoted by t_{pr} , versus the radius of the TX by searching the highest value in (5) and recording the corresponding time. First, we observe that the time to reach the peak release probability increases with an increase in r_T . This is because a vesicle needs to diffuse for longer to arrive at the TX membrane with a larger radius. Second, by comparing parameter sets 1), 2), and 3), we observe that the time increases with a decrease in k_f . This is because lower k_f reduces the fusion probability such that it takes longer to reach the peak release probability. Third, by comparing parameter sets 1), 4), and 5), we observe that the time increases with a decrease in D_v . This is because the smaller value of D_v slows down the



(a) Releasing probability



(b) The number of molecules released

Fig. 2. Molecule release probability from the MF-based TX at time t and the number of molecules released from the MF-based TX by time t versus time t for three parameter sets.

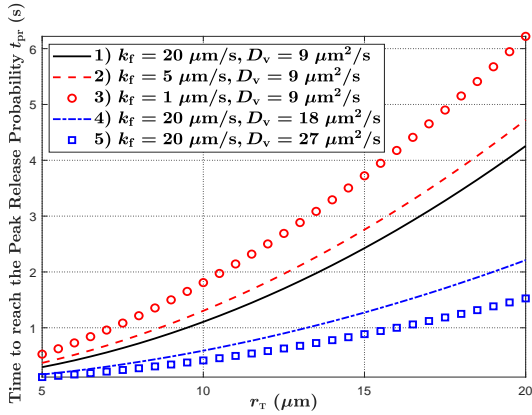


Fig. 3. Time to reach the peak molecule release probability from the TX versus r_T for five parameter sets.

vesicle such that a longer time is required for the vesicle to arrive at the TX membrane.

In Fig. 4, we plot the end-to-end hitting probability of molecules at the RX at time t versus time t . First, by comparing parameter sets 1) and 2), we observe that the peak end-to-end hitting probability decreases with a decrease in k_f . This is because decreasing k_f reduces the release probability of molecules such that the end-to-end hitting probability at the RX decreases. Second, by comparing parameter sets 1) and

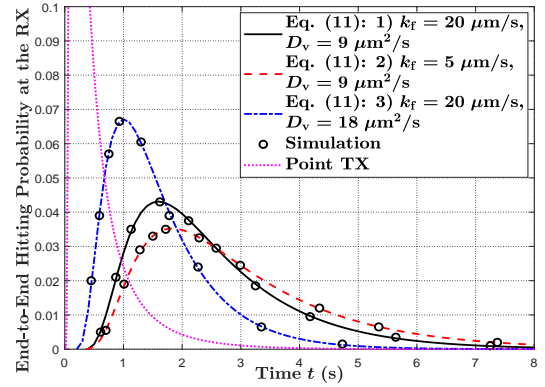


Fig. 4. End-to-end hitting probability of molecules at the RX at time t versus time t for three parameter sets.

3), we observe that the peak end-to-end hitting probability increases and less time is required for molecules to start hitting the RX with an increase in D_v . This is because the larger value of D_v enables the earlier release of molecules and increases the peak release probability. Third, to show the difference between the MF-based TX and an ideal point TX, we also plot the hitting probability of an ideal point TX based on [19, eq. (9)]. We observe that the peak value of the hitting probability curve for the point TX is larger than that for the MF-based TX, i.e., the hitting probability curve for the point TX is narrower. This is because molecules are instantaneously released from the point TX while molecules need to be transported to TX membrane before release.

VI. CONCLUSION

In this paper, we proposed a new TX model that are based on MF between vesicles generated within the TX and the TX membrane to release molecules. We derived the molecule release probability and the fraction of released molecules from the TX. By considering a fully-absorbing RX in the environment, we derived new closed-form expressions for the end-to-end molecule hitting probability at the RX. We further propose a simulation framework for the MF-based TX. Our results showed that our analytical expressions are accurate. They also showed that a low MF probability or low vesicle mobility slows the release of molecules, extends the time to reach the peak release probability, and reduces the end-to-end molecule hitting probability at the RX. Future work includes 1) considering the reflecting membrane of the TX and 2) investigating the scenario with mobile TX and RX.

APPENDIX A

PROOF OF THEOREM 1

Using separation of variables [21], we express $C(r, t)$ as $C(r, t) = R(r)T(t)$, where $R(r)$ and $T(t)$ are functions of r and t , respectively. Substituting $C(r, t)$ into (3), we obtain

$$\frac{2D_v R'(r)}{rR(r)} + \frac{D_v R''(r)}{R(r)} = \frac{T'(t)}{T(t)} \stackrel{(a)}{=} \epsilon, \quad (17)$$

where $R'(r) = \frac{\partial R(r)}{\partial r}$, $R''(r) = \frac{\partial^2 R(r)}{\partial r^2}$, and $T'(t) = \frac{\partial T(t)}{\partial t}$. The left-hand side of the first equality in (17) is a function of

r , denoted by $\epsilon(r)$, and the right-hand side is a function of t , denoted by $\epsilon(t)$. As $\epsilon(r) = \epsilon(t)$, $\epsilon(r)$ and $\epsilon(t)$ are constant ϵ that results in the equality (a). Based on (17), we first obtain

$$r^2 R''(r) + 2rR'(r) - \frac{\epsilon}{D_v} r^2 R(r) = 0. \quad (18)$$

By setting $\epsilon = -D_v \lambda_n^2$, $n = 1, 2, 3, \dots$, (18) becomes the Bessel function [22]. For each given λ_n , the solution of $R(r)$ in (18), denoted by $R_n(r)$, is given by $R_n(r) = E_n j_0(\lambda_n r)$, where E_n is a constant. As $R_n(r)$ needs to satisfy the boundary condition in (4), we substitute $R_n(r)$ into (4) and obtain (6). Based on (17), we then obtain $\frac{T_n'(t)}{T_n(t)} = -D_v \lambda_n^2$. By considering an obvious condition $T_n(t \rightarrow \infty) = 0$, one principle solution to $T_n(t)$ is $T_n(t) = B_n \exp(-D_v \lambda_n^2 t)$. Based on the principle of superposition, $C(r, t)$ then becomes $C(r, t) = \sum_{n=1}^{\infty} R_n(r) T_n(t) = \sum_{n=1}^{\infty} E_n B_n j_0(\lambda_n r) \exp(-D_v \lambda_n^2 t)$.

We next determine $E_n B_n$ based on the initial condition in (2). According to [15, eq. (12)] and [12, eq. (21)], if $n \neq n'$, $r j_0(\lambda_n r)$ and $r j_0(\lambda_{n'} r)$ are orthogonal to each other. We then derive $\int_0^{r_T} r^2 j_0(\lambda_n r) j_0(\lambda_{n'} r) dr$ as

$$\int_0^{r_T} r^2 j_0(\lambda_n r) j_0(\lambda_{n'} r) dr = \begin{cases} 0, & n \neq n', \\ \frac{2\lambda_n r_T - \sin(2\lambda_n r_T)}{4\lambda_n^3}, & n = n'. \end{cases} \quad (19)$$

We substitute $C(r, t)$ into (2), and then multiply $j_0(\lambda_n r)$ to both sides of the equality. With some mathematical manipulations and taking the integral of both sides with respect to r , we obtain

$$\sum_{n=1}^{\infty} E_n B_n \int_0^{r_T} r^2 j_0^2(\lambda_n r) dr = \frac{1}{4\pi} \int_0^{r_T} \delta(r) j_0(\lambda_n r) dr. \quad (20)$$

Based on (19) and (20), we obtain $E_n B_n = \frac{\lambda_n^3}{\pi(2\lambda_n r_T - \sin(2\lambda_n r_T))}$, and then obtain $C(r, t)$ accordingly. Based on [23, eq. (3.106)], the vesicle fusion probability, which is also the release probability of molecule σ , is expressed as $f_r(t) = 4\pi r_T^2 k_f C(r_T, t)$. By substituting $C(r_T, t)$ into $f_r(t)$, we obtain (5).

APPENDIX B PROOF OF LEMMA 1

We perform the surface integral by considering a small surface element that is the lateral surface of a conical frustum, denoted by dS , on the TX membrane. The point α is on dS with the coordinates (x, y, z) . The base and top radii of this conical frustum are y and $y + dy$, respectively, and the slant height is $\sqrt{d^2 x + d^2 y}$. Based on the expression for the lateral surface area of a conical frustum, dS is calculated as $dS = 2\pi y \sqrt{1 + \left(\frac{dy}{dx}\right)^2} dx + \pi \frac{dy}{dx} \sqrt{1 + \left(\frac{dy}{dx}\right)^2} d^2 x$. Since $y = \sqrt{r_T^2 - x^2}$, we have $\frac{dy}{dx} = -\frac{x}{\sqrt{r_T^2 - x^2}}$. By substituting $\frac{dy}{dx}$ into dS , we obtain $dS = 2\pi r_T dx - \frac{\pi x r_T}{r_T^2 - x^2} d^2 x \approx 2\pi r_T dx$, where $\frac{\pi x r_T}{r_T^2 - x^2} d^2 x$ is omitted since it is the higher order infinitesimal. As dS is infinitesimal, we treat the distance between each point on dS and the center of the RX as l_α , where l_α can be expressed based on x as $l_\alpha = \sqrt{r_T^2 + l^2 - 2lx}$.

By substituting l_α into (8), we obtain $p_\alpha(t, x)$. Accordingly, the hitting probability at the RX for molecules released from dS is $\rho p_\alpha(t, x) dS$. Furthermore, $p_u(t)$ is obtained by integrating $\rho p_\alpha(t, x) dS$, i.e., $p_u(t) = \int_{-\Omega_T}^{\Omega_T} \rho p_\alpha(t, x) dS = \int_{-r_T}^{r_T} 2\pi r_T \rho p_\alpha(t, x) dx$. By substituting $p_\alpha(t, x)$ into $p_u(t)$ and solving the integral, we obtain (9).

REFERENCES

- [1] N. Farsad, H. B. Yilmaz, A. Eckford, C.-B. Chae, and W. Guo, "A comprehensive survey of recent advancements in molecular communication," *IEEE Commun. Surveys Tuts.*, vol. 18, no. 3, pp. 1887–1919, 3rd Quarter, 2016.
- [2] A. Ahmadzadeh, H. Arjmandi, A. Burkovski, and R. Schober, "Comprehensive reactive receiver modeling for diffusive molecular communication systems: Reversible binding, molecule degradation, and finite number of receptors," *IEEE Trans. Nanobiosci.*, vol. 15, no. 7, pp. 713–727, Oct. 2016.
- [3] V. Jamali, A. Ahmadzadeh, W. Wicke, A. Noel, and R. Schober, "Channel modeling for diffusive molecular communication—a tutorial review," *Proc. IEEE*, Jun. 2019.
- [4] H. B. Yilmaz, G.-Y. Suk, and C.-B. Chae, "Chemical propagation pattern for molecular communications," *IEEE Wireless Commun. Lett.*, vol. 6, no. 2, pp. 226–229, Apr. 2017.
- [5] H. Arjmandi, A. Ahmadzadeh, R. Schober, and M. N. Kenari, "Ion channel based bio-synthetic modulator for diffusive molecular communication," *IEEE Trans. Nanobiosci.*, vol. 15, no. 5, pp. 418–432, Jul. 2016.
- [6] M. Schäfer, W. Wicke, W. Haselmayr, R. Rabenstein, and R. Schober, "Spherical diffusion model with semi-permeable boundary: A transfer function approach," in *Proc. IEEE ICC*, Jun. 2020, pp. 1–7.
- [7] R. Jahn and T. C. Südhof, "Membrane fusion and exocytosis," *Annu. Rev. Biochem.*, vol. 68, no. 1, pp. 863–911, Jul. 1999.
- [8] A. Morgan, "Exocytosis," *Essays BioChem.*, vol. 30, pp. 77–95, 1995.
- [9] J. S. Bonifacio and B. S. Glick, "The mechanisms of vesicle budding and fusion," *Cell*, vol. 116, no. 2, pp. 153–166, Jan. 2004.
- [10] M. Kyoung and E. D. Sheets, "Vesicle diffusion close to a membrane: intermembrane interactions measured with fluorescence correlation spectroscopy," *Biophys. J.*, vol. 95, no. 12, pp. 5789–5797, Dec. 2008.
- [11] J. C. Hay, "Calcium: a fundamental regulator of intracellular membrane fusion?" *EMBO Rep.*, vol. 8, no. 3, pp. 236–240, Mar. 2007.
- [12] H. Arjmandi, M. Zoofaghari, and A. Noel, "Diffusive molecular communication in a biological spherical environment with partially absorbing boundary," *IEEE Trans. Commun.*, vol. 67, no. 10, pp. 6858–6867, Jul. 2019.
- [13] R. Erban and S. J. Chapman, "Reactive boundary conditions for stochastic simulations of reaction–diffusion processes," *Physical Biology*, vol. 4, no. 1, p. 16, 2007.
- [14] R. Chang, *Physical Chemistry for the Biosciences*. Sausalito, CA, USA: Univ. Science Books, 2005.
- [15] F. Dinç, B. C. Akdeniz, A. E. Pusane, and T. Tugcu, "Impulse response of the molecular diffusion channel with a spherical absorbing receiver and a spherical reflective boundary," *IEEE Trans. Mol. Biol. Multi-Scale Commun.*, vol. 4, no. 2, pp. 118–122, Jun. 2018.
- [16] H. C. Berg, *Random Walks in Biology*. Princeton, NJ, USA: Princeton Univ. Press, 1993.
- [17] J. Crank, *The Mathematics of Diffusion*. London, U.K.: Oxford Univ. Press, 1979.
- [18] F. W. Olver and L. C. Maximon, *Bessel Functions*. New York, NY: Cambridge Univ. Press, 1960.
- [19] A. C. Heren, H. B. Yilmaz, C.-B. Chae, and T. Tugcu, "Effect of degradation in molecular communication: Impairment or enhancement?" *IEEE Trans. Mol. Biol. Multi-Scale Commun.*, vol. 1, no. 2, pp. 217–229, Jun. 2015.
- [20] A. Noel, K. C. Cheung, R. Schober, D. Makrakis, and A. Hafid, "Simulating with AcCoRD: Actor-based communication via reaction–diffusion," *Nano Commun. Netw.*, vol. 11, pp. 44–75, Mar. 2017.
- [21] K. Cole, J. Beck, A. Haji-Sheikh, and B. Litkouhi, *Heat Conduction Using Greens Functions*. Boca Raton, FL, USA: CRC Press, 2010.
- [22] R. Beals and R. Wong, *Special Functions and Orthogonal Polynomials*. Cambridge, U.K.: Cambridge Univ. Press, 2016, vol. 153.
- [23] K. Schulten and I. Kosztin, *Lectures in Theoretical Biophysics*. Univ. Illinois, Champaign, IL, USA, 2000, vol. 117.